

THE TWO PHASE, TWO PLUG REACTOR THE SEPARATE PHASE RESIDENCE TIMES EFFECT

Colin McGreavy
The University of Leeds, Chem. Eng. Dept.
Leeds LS2 9JT, UK

Marcos Sugaya
Petrobras S.A., Cenpes
Rio de Janeiro 21910-900, Brazil

KEYWORDS: Delayed coking, visbreaking, pyrolysis

ABSTRACT

The two phase, two plug flow reactor (2TP-R) is a distinctive example which highlights the problems in modeling complex multiphase flows where the different phases can have well-defined and independent residence times which need to be taken into account. As a case study, the pyrolysis of distillation residues in a 2TP-R scheme is examined to illustrate some of the issues in characterizing such systems which include practical applications such as visbreaking and delayed coking furnaces and other residue upgrading processes. Kinetic parameters for the lumped pseudocomponents system have been derived from isothermal pilot plant runs. Operating parameters and geometric considerations have been examined aiming at maximization of the light derivatives in the pyrolysis of residues. It is important to balance the conversion between the furnace and the soaking drums downstream to optimize the yield of products and the overall operation.

INTRODUCTION

Delayed coking furnaces are designed to postpone chemical transformations in the feed to the soaking drums downstream so as to avoid deposition of coke in the furnace tubes which would limit the campaign time. High velocities, moderate heat fluxes and large surface/diameter ratios are necessary to accomplish this.

Generally, a box geometry with two radiant sections connected to a single convection section is used. The tubes are horizontal and, in the radiant section, they are often located adjacent to the walls but separated on a large pitch in order to improve the distribution of heat. More recently the distribution of heat has been enhanced by placing the tubes in a double fired zone at the center of the radiant boxes with the feed flowing downwards in a direction opposite to the flow of combustion gases. This has the advantage of reducing the maximum wall temperatures.

Not all of the tube length is used for heat exchange. Dead end sections are usually connected by 'mule-ear' heads to one side of the furnace with 'U' sections at the opposite side. These configurations give rise to significant pressure drops while adding to the soaking volume. A variety of tube lengths, diameters and pitches is also used.

Kinetic constants for chain initiation reactions in the liquid and vapor phases are related by the equation

$$K_{liq} = k_{vap} \cdot \exp\left(\frac{\Delta S^{\otimes}}{R} - \frac{\Delta H^{\otimes}}{RT}\right) \quad \text{Equation 1}$$

where ΔS^{\otimes} and ΔH^{\otimes} are the differences in the entropy and enthalpy of the activated complex and reactants in the liquid and vapor phases (1). Since ΔH^{\otimes} is negative, reactions in the vapor phase can be neglected at the low temperatures used in delayed coking, visbreaking and similar processes.

The generation of vapor in the process influences the residence time of the liquid phase because it effectively reduces the volume. Steam can be used to reduce the partial pressure of the hydrocarbons in the vapor phase and hence increase the vaporization which enables the residence times to be controlled. This arrangement results in increased flexibility for a particular geometry. When estimating residence times, it is therefore important to consider a distinction between the liquid holdup in the coil and the vapor/liquid ratio which is determined by phase equilibrium.

APPROACH

The model uses lumped kinetic parameters derived from pilot plant experiments. The liquid phase holdup can be estimated using the method due to Hughmark (2). As the hydrocarbon vaporizes, the flow regime along the tubes changes. Baker's map (3) can be used to follow the changes. Phase equilibrium is based on the Redlich-Kwong equation as modified by Soave (4). The physical properties have been estimated using the method due to Dean-Stiel (vapor viscosity), Twu (liquid viscosity), Mallan *et al.* (liquid conductivity), Stiel-Thodos (vapor conductivity) and Gunn-Yamada-Rackett (liquid density). The temperature dependence of liquid viscosities is obtained from the ASTM procedure modified by Wright (5), using appropriate mixing rules. Single phase pressure drop is calculated using the equation due to Chen (6). For two phase flow, the method of Dukler (7) and a proprietary correlation (8) have been used.

A mass balance is given by

$$\frac{dc_{i,T}}{dx} = -\frac{h_L A_T \rho_L}{W_T} k_i c_{i,L} \quad \text{Equation 2}$$

where c_i stands for the concentration of species i , h the holdup, A the cross-sectional area, W the mass flow rate, ρ the density, k the kinetic constant and the subscripts L and T denote the liquid phase and the total stream respectively.

Enthalpies are calculated based on the Lee-Kesler equations and the heat of reaction is taken as 800 J/kg for products boiling below 204 C (ASTM D-86). Wall temperatures are estimated from the heat flux and adopting the definition of heat transfer coefficients and the methodology described in API RP-530 (1988).

The 2TP model used here has been extended to take account of the transfer line between the furnace and the coking drums with pipe fittings accounted for by using appropriate equivalent lengths.

Change in the static head is based based on the following equation

$$\left(\frac{dP}{dx}\right)_d = (h_L \rho_L + h_V \rho_V) \sin \theta \quad \text{Equation 3}$$

where P is the pressure and θ is the inclination to the vertical. The flow regime is taken from the zones defined by Griffith and Wallis (9).

RESULTS AND DISCUSSION

The furnaces at Petrobras Gabriel Passos Unit 52 have two radiation chambers connected to a single convection section with the feed being split into four passes per furnace. Tubes in the radiation boxes are in two horizontal lines near the walls fired from the center and each furnace feeds a pair of coke drums. Geometric data are presented in Table 1, operating conditions in Table 2. Table 3 contains a geometric description of the transfer line.

Table 4 compares the simulation results with process data. Furnace B generates more coke than A, as indicated by the measured pressure drop, which is 30 % higher. The campaign time is not reported, although furnace A has recently been decoked. The calculated pressure drop in B needs to be increased by 23% to reproduce this effect. Correspondingly, A needs to be reduced by 31% to match the plant pressure drop. This means that the pressure drop correlation is conservative as far as design is concerned.

The heat duty and fuel gas consumption matches the plant data very well (Table 4). In Figures 1-2 the temperature of the tubes predicted by the model compare well with the plant and the agreement between the model output and the process data is generally good.

In Figure 3, the composition profile in furnace A is represented by the fraction of products boiling below 350 C. As can be seen, reaction is significant only in the final third of the tubes, where the temperature is above 400 C. No significant reaction occurs in the convection zone. Higher coke drum temperatures favor condensation reactions at the expense of cracking, because of the different activation energies. However this also increases the vaporization in the drums causing in a net decrease in coke production.

The choice of appropriate operating conditions is crucial in seeking to increase the production of liquids and needs to be anticipated at the design stage because more options are available at this time. In particular, a low operating pressure is very desirable since it decreases the production of coke.

Table 5 shows that an important fraction of the conversion and pressure drop arise in the transfer line between the furnace and the coking drums. In fact, most of the conversion and pressure drop takes place at the last third of the coil in the furnace. Clearly, efforts to reduce the

system pressure should be directed to these sections in particular by minimizing the length of the transfer lines and the number of pipe fittings, which depend on plant layout.

CONCLUSIONS

Good delayed coking furnace performance is generally seen as meeting the specified outlet temperatures for the lowest possible conversion since this would mean that the campaign time is maximized. However, the energy required for the endothermic chemical reactions and vaporization of products in the coke drums is supplied by the furnace. If the conversion upstream the drums is low, the temperature needs to be increased to ensure that a similar yield of liquids is obtained. In practice this increases the tendency of coking in the furnace tubes, since higher wall temperatures have to be expected. It can also result in shot coke formation (10).

The goal should not be to minimize conversion in the furnace but to reduce the pressure drop. This vaporizes products at the lowest possible temperature, transferring energy to the drums as latent rather than sensible heat. Tube coking is minimized by using high velocities while not reducing residence times, e.g., by using small diameters and longer coil lengths.

The scope for gaining maximum benefit using this approach is obviously increased if the process models can be further developed. This requires a good representation of the angular distribution of heat in the tubes.

REFERENCES

1. Bozzano G. Tesi di Dottorato in Ingegneria Chimica 1994, Politecnico di Milano.
2. Hughmark G. A. Chemical Engineering Progress 1962, 62.
3. Baker O. Oil & Gas Journal 1954, July 26, 185.
4. Soave G., Chemical Engineering Science 1972, 27, 1197.
5. Wright W. A. Journal of Materials 1969, 4, 1, 19.
6. Chen N. H. Ind. Eng. Chem. Fund. 1979, 18, 296.
7. Dukler A. E.; Wicks M.; Cleveland R. G. AIChE Journal 1964, 44.
8. Sugaya M. F.; Maciel R. Petrobras Internal Report 1994.
9. Griffith P.; Wallis G. B. Journal of Heat Transfer 1961, Aug., 307.
10. Ellis P. J.; Bacha J. D. Light Metals 1996, 477.
11. Dean D. E.; Stiel L. I. AIChE Journal 1965, 526.
12. Gunn R. D.; Yamada T. AIChE Journal 1971, 17, 1341.
13. Mallan G. M.; Michaelian M. S.; Lockhart F. J. J. Chem. Eng. Data 1972, 17, 412.
14. Stiel L. I., Thodos G., AIChE Journal 1964, Jan., 26.

Table 1 Geometric data for tubes in furnaces 52-F-1 A/B. Dead ends are 2 x 225 mm.

Section	Part	L_{eff} (m)	d_i (mm)	d_o (in)	Avg. pitch (mm)	Tubes (per pass)
Convection	1-4	10.364	74	89	189	38
Radiation	1	10.364	65	83	199	34

Table 2 Operating data for furnaces 52-F-1 (including a 10 % heavy gasoil recycle).

Furnace	Pass	Combined feed (m ³ /d)	Water (m ³ /d)
A	1	320	3.5
	2	316	3.5
	3	318	3.4
	4	313	3.4
B	1	315	3.5
	2	316	3.5
	3	315	3.5
	4	316	3.5
total		2530	27.8

Table 3 Transfer line geometry up to the switch valve.

Part	Type	d _{in} (in)	d _{out} (in)	Length (m)	Inclination (degrees)	Passes
1	nozzle	3	3	-	-	4
2	expansion	3	4	-	-	4
3	line	4	4	2.2	0	4
4	cross	4	4	-	-	4
5	line	4	4	1.2	0	4
6	expansion	4	6	-	-	4
7	cross	6	6	-	-	2
8	line	6	6	1.0	90	2
9	cross	6	6	-	-	2
10	line	6	6	2.0	0	2
11	expansion	6	8	-	-	2
12	cross	8	8	-	-	1
13	line	8	8	11.7	0	1
14	cross	8	8	-	-	1
15	line	8	8	7.7	90	1
16	cross	8	8	-	-	1
17	line	8	8	2.3	0	1

Table 4 Results of the model in comparison with industrial data. Pressures in bars, temperatures in C, duties in 10⁶ kcal/h and fuel gas consumption in Nm³/d.

	52-F-1 A	Model	52-F-1 B	Model
T _{in, convection}	238	238	238	238
T _{out, convection}	396	396	372	372
Duty _{convection}	n.a.	6.2	n.a.	5.2
T _{out, radiation}	502	502	502	503
Duty _{radiation}	n.a.	5.7	n.a.	6.5
Duty _{furnace}	11.1	11.9	11.5	11.7
Fuel gas	1380	1470	1420	1450
T _{switch valve}	n.a.	490	n.a.	490
P _{in, furnace}	16.2	16.2	19.9	19.9
P _{in, convection}	14.7	14.7	18.4	18.4
P _{out, convection}	n.a.	13.6	n.a.	16.8
ΔP _{convection}	n.a.	1.1	n.a.	1.6
P _{in, radiation}	n.a.	13.6	n.a.	16.8
P _{out, radiation}	n.a.	8.5	n.a.	10.1
ΔP _{radiation}	n.a.	5.1	n.a.	6.7
ΔP _{furnace}	n.a.	7.7	n.a.	9.8
P _{switch valve}	4.0	4.1	4.3	4.2
ΔP _{transfer line}	n.a.	4.4	n.a.	5.9
ΔP _{furnace+tr.in.}	12.2	12.1	15.6	15.7

Table 5 Distribution of conversion and pressure drop in the system.

	52-F-1 A	52-F-1 B
conversion in furnace	83 %	81 %
conversion in transfer line	17 %	19 %
ΔP _{furnace}	64 %	62 %
ΔP _{transfer line}	36 %	38 %

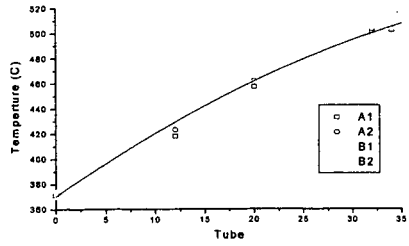


Figure 1 Fluid temperatures in the radiation zones A/B of F-1 A.

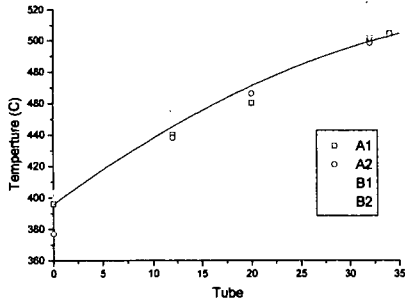


Figure 2 Fluid temperatures in the radiation zones A/B of F-1 B.

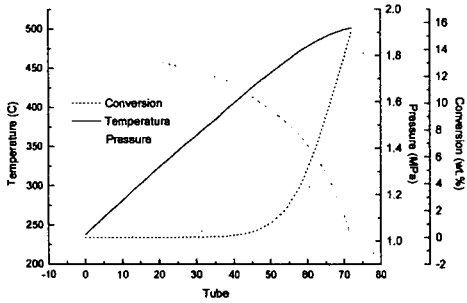


Figure 3 Conversion in F-1 A. The radiation section starts after tube 34.